

Pre-Steady-State Analysis of ATP Hydrolysis by *Saccharomyces cerevisiae* DNA Topoisomerase II. 2. Kinetic Mechanism for the Sequential Hydrolysis of Two ATP[†]

Timothy T. Harkins,^{‡,||} Timothy J. Lewis,[§] and Janet E. Lindsley^{*,‡}

Department of Biochemistry, University of Utah School of Medicine, 50 North Medical Drive, Salt Lake City, Utah 84132, and Department of Mathematics, University of Utah, 233 John Widtsoe Building, Salt Lake City, Utah 84112

Received November 26, 1997; Revised Manuscript Received March 17, 1998

ABSTRACT: In the preceding paper, we showed that DNA topoisomerase II from *Saccharomyces cerevisiae* binds two ATP and rapidly hydrolyzes at least one of them before encountering a slow step in the reaction mechanism. These data are potentially consistent with two different types of reaction pathways: (1) sequential ATP hydrolysis or (2) simultaneous hydrolysis of both ATP. Here, we present results that are consistent only with topoisomerase II hydrolyzing its two bound ATP sequentially. Additionally, these results indicate that the products of the first hydrolysis are released from the enzyme before the second ATP is hydrolyzed. Release of products from both the first and second hydrolyses contributes to the rate-determining process. The proposed mechanism for ATP hydrolysis by topoisomerase II is complex, having nine rate constants. To calculate values for each of these rate constants, a technique of kinetic parameter estimation was developed. This technique involved using singular perturbation theory in order to estimate rate constants, and consequently identify kinetic steps following the rate-determining step.

For catalytic turnover, type II DNA topoisomerases must bind and hydrolyze ATP in order to transport one DNA duplex through a transient break in another [for recent reviews, see (1, 2)]. The kinetic mechanism for this ATPase reaction was previously unknown. We showed in the preceding paper that the topoisomerase II homodimer binds two ATP and rapidly hydrolyzes at least one. These data are consistent with two different mechanisms, as shown in Scheme 1.

Data from these previous experiments could neither disprove one of these pathways nor provide information on the steps of product release. Additionally, the rate-determining step was not identified. The combination of steady-state and pre-steady-state studies presented in this paper defines a favored reaction pathway for ATP hydrolysis by topoisomerase II. The mathematical technique of singular perturbation, coupled with the use of a minimization program, was used to determine rate constants for each step of the pathway.

MATERIALS AND METHODS

Materials. Standard reagents were purchased from the following commercial resources: ATP, Pharmacia; [α -³²P]-ATP (3000 Ci/mmol), New England Nuclear; ultrapure HEPES,¹ Boehringer Mannheim; [2,8-³H]AMPPNP¹ (21 Ci/mmol), ICN; NADH, phospho(enol)pyruvate (PEP, trisodium salt hydrate), and pyruvate kinase (700 units/mL)/lactate dehydrogenase (100 units/mL) from rabbit muscle, sodium orthovanadate, Sigma. The *Saccharomyces cerevisiae* topoisomerase II and the sheared salmon sperm DNA were purified as described in the preceding paper. [α -³²P]ADP was made by reacting [α -³²P]ATP with topoisomerase II/DNA; the [α -³²P]ADP was purified as previously described (3). All reactions were performed in the same reaction buffer [50 mM HEPES–KOH (pH 7.5), 150 mM KOAc, and 10 mM Mg(OAc)₂], except for the pH–rate studies, as described below. All buffers were filtered (0.45 μ m).

Steady-State Product Inhibition Studies. A discontinuous assay involving the conversion of [α -³²P]ATP to [α -³²P]ADP was used as described in the preceding paper. Reactions (100 μ L final) performed in the presence of DNA (25 μ M base pairs) included 100 nM topoisomerase II dimer; those done in the absence of DNA contained 200 nM enzyme dimer. The indicated concentration of inhibitor was mixed with this solution, and the reactions were initiated by addition of [α -³²P]ATP (30 Ci/mmol). The final ATP concentrations

[†] This work was supported by Grant GM51194 from the National Institutes of Health, and in part by a grant from the Lucille P. Markey Charitable Trust. T.T.H. was supported in part by NCI Training Grant CA09602-06. T.J.L. was supported in part by NFS Grant DMS-9626334. J.E.L. was supported in part by ACS Grant JFRA-622.

* To whom correspondence should be addressed. E-mail: jlindsley@msscc.med.utah.edu. FAX: (801) 581-7959.

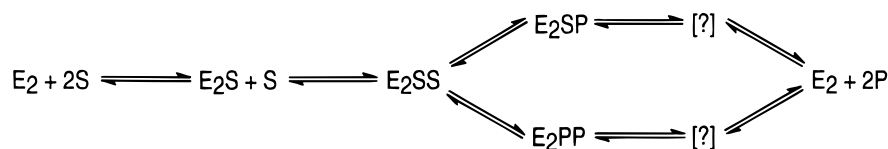
[‡] Department of Biochemistry, University of Utah School of Medicine.

[§] Department of Mathematics, University of Utah.

^{||} Present address: Molecular Informatics, Incorporated, 1800 Old Pecos Trail, Suite M, Santa Fe, NM 87505.

¹ Abbreviations: AMPPNP, adenosine 5'-(β , γ -imidotriphosphate); HEPES, *N*-(2-hydroxyethyl)piperazine-*N'*-2-ethanesulfonic acid; PEP, phospho(enol)pyruvate; P_i, inorganic phosphate.

Scheme 1



ranged from 50 μM to 1.5 mM. Aliquots (10 μL) were withdrawn at various time points and quenched with EDTA/SDS (50 mM/1% final concentrations). The concentration of ADP produced at each time point was determined in triplicate as described in the preceding paper. The rates of ATP hydrolysis were calculated from ADP concentrations determined at seven time points ranging from 15 s to 30 min, including a minus enzyme time point.

Pre-Steady-State Inhibition with Vanadate. Chemical quench and pulse–chase experiments were performed and analyzed as described in the preceding paper, except that where indicated 100 μM vanadate was included in the sample loop containing ATP. The time courses compared were all performed on the same day, with the same topoisomerase II/DNA preparation.

Pre-Steady-State ADP Protection Assay. To determine the amount of ADP bound to topoisomerase II during the pre-steady-state, the concentration of ADP protected from conversion back to ATP by pyruvate kinase and PEP was measured, and will be referred to as an ADP protection assay (4). These chemical quench assays were done as described in the preceding paper, except that in the indicated reaction 542 units/mL pyruvate kinase and 20 mM PEP were included in the sample loop with the ATP. For comparison, a standard chemical quench assay, except that 20 mM PEP was included in the ATP solution, was performed using the same topoisomerase II/DNA preparation. Two important control reactions were also performed. The first control involved showing that the above concentrations of pyruvate kinase and PEP could convert free ADP to ATP faster than topoisomerase II could release ADP. For this control, pyruvate kinase and PEP were placed in one sample loop, and 100 μM [α - ^{32}P]ADP was placed in the other sample loop. These were mixed and quenched at time points between 5 and 100 ms using our standard chemical quench [250 mM EDTA in 100 mM Tris (pH 10), followed by 1% SDS]. It was found that the rate of conversion of ADP back to ATP by pyruvate kinase was 10-fold greater than the rate of ADP release by topoisomerase II (data not shown). The second control involved showing that our standard chemical quench rapidly inactivates pyruvate kinase. Pyruvate kinase and PEP were placed in one sample loop, the EDTA/Tris quench solution was placed in the second sample loop, and [α - ^{32}P]ADP was placed in the quench line. When the enzyme and quench were mixed for as short as 3 ms prior to addition of the ADP, no conversion of ADP to ATP could ever be detected (data not shown). Therefore, the quench inactivates pyruvate kinase within 3 ms.

ATPase Rate Profiles as a Function of pH. A buffer was used for these studies that has a constant ionic strength over the range of pH studied (5.3–9.6) (5). The stock for this buffer contained 33 mM succinic acid, 44 mM imidazole, and 44 mM diethanolamine, and the pH was adjusted with either KOH or acetic acid as necessary. This buffer was shown to have no inhibitory effects on topoisomerase II.

Additionally, the enzyme was completely stable at each pH for at least 1 h. The final reactions contained 50 mM buffer, 175 mM KOAc, and 10 mM $\text{Mg}(\text{OAc})_2$. Assays performed in the presence of DNA contained 100 nM topoisomerase II dimer and 50 μM pHc624 DNA (base pairs) (6); in the absence of DNA, 500 nM topoisomerase II was used. A coupled assay using pyruvate kinase, PEP, lactate dehydrogenase, and NADH was used to determine the rates of ATP hydrolysis at each pH for 10 ATP concentrations ranging from 30 μM to 2 mM (7). At each pH used, the enzymes in the coupling system were shown to function much more rapidly than topoisomerase II could hydrolyze ATP. The pH reported is that measured at the end of the reactions; however, in no case was there a significant change in pH during the reaction. The reactions and pH measurements were done at 25 $^\circ\text{C}$. For simplicity, the positive cooperativity detected at low ATP concentrations was ignored in this analysis, and the approximate values for V_{max} and V_{max}/K_m were determined by fitting the initial velocities at 10 ATP concentrations to the Michaelis–Menten equation.

Data Analysis. Steady-state ATPase and pH data were fit to the Michaelis–Menten equation using Grafit version 3.0 (Erithacus software). Pre-steady-state vanadate inhibition data were fit to single-exponential equations with a linear term, $A(1 - e^{-Bt}) + Ct$, using SigmaPlot version 3.0 (Jandel software). Parameter estimation was attained by analytical methods using singular perturbation theory (8). Reaction mechanisms were simulated, and values for the rate constants were minimized using a variable time step Euler method (code was written in Fortran) (9). The χ^2 -minimization routine used a biased random walk in parameter space in order to find an optimum fit.

RESULTS

Order of Product Release. To determine the kinetic mechanism for ATP hydrolysis by topoisomerase II, the order in which the products, ADP and P_i , are released from the enzyme was elucidated. Steady-state product inhibition profiles can be used to predict the order of product release. The initial rates of ATP hydrolysis at varying ATP and ADP concentrations are shown for reactions performed in the presence of DNA (Figure 1A) or the absence of DNA (Figure 1B). These data were fit to a simple competitive inhibition model, ignoring potential interactions at the two ATPase sites. The calculated K_i values for ADP are $80 \pm 10 \mu\text{M}$ and $170 \pm 30 \mu\text{M}$, in the presence and absence of DNA, respectively. Although this fit is only an approximation, these data cannot be fit by either a noncompetitive or an uncompetitive model for inhibition. While there is good evidence for positive cooperativity in ATP binding, any cooperativity between ATP and ADP, or between two ADP, has not been determined. Therefore, it is not possible to fit these data to a complex two-site model involving competitive inhibition and cooperativity (10). These data are most

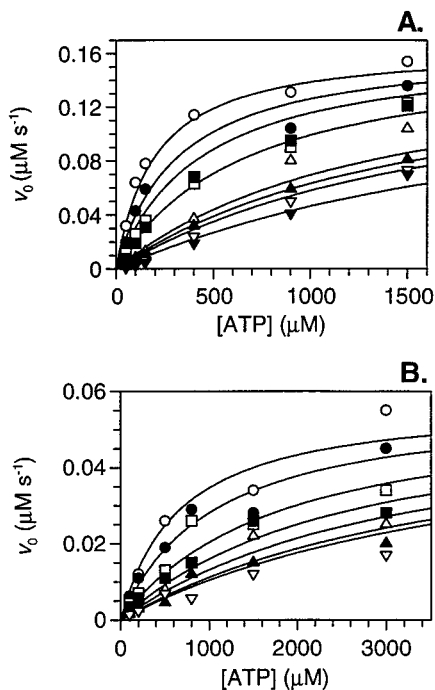


FIGURE 1: ADP is a competitive inhibitor of ATP hydrolysis by topoisomerase II both in the presence (A) and the absence (B) of DNA. In both cases, the initial velocities determined by discontinuous ATPase analysis are fit to an equation describing simple competitive inhibition: $v_o = (V_{\max}[S]/\{K_m(1 + [I]/K_i) + [S]\})$. (A) The ADP concentrations used in the presence of DNA were 0 (\circ), 50 (\bullet), 100 (\square), 200 (\blacksquare), 500 (\triangle), 600 (\blacktriangle), 700 (∇), and 1000 μM (\blacktriangledown). (B) In the absence of DNA, the inhibitor concentrations were 0 (\circ), 100 (\bullet), 300 (\square), 500 (\blacksquare), 700 (\triangle), 900 (\blacktriangle), and 1000 μM (∇). The calculated values for $K_{i(\text{ADP})}$ and $K_{m(\text{ATP})}$ in the presence of DNA are $80 \pm 10 \mu\text{M}$ and $200 \pm 30 \mu\text{M}$, respectively. In the absence of DNA, the calculated values for $K_{i(\text{ADP})}$ and $K_{m(\text{ATP})}$ are $170 \pm 30 \mu\text{M}$ and $660 \pm 130 \mu\text{M}$, respectively.

consistent with ADP competing with ATP for binding to topoisomerase II. In other words, these inhibition data are not consistent with a mechanism having ADP binding to an enzyme–inorganic phosphate complex, suggesting that P_i is released from the enzyme prior to ADP.

Inorganic phosphate is a very poor inhibitor of topoisomerase II; preliminary data suggest that the K_i for P_i is on the order of 100 mM (data not shown). Because such high concentrations of P_i affect the ionic strength of the reaction, a more accurate determination could not be made. However, vanadate, a P_i mimic, is a potent inhibitor of topoisomerase II. Vanadate is a dead-end inhibitor of many ATPases, and is thought to bind and stabilize the enzyme–ADP complex, preventing product dissociation (11, 12). Initial velocity data of ATP hydrolysis by topoisomerase II in the presence of various ATP and vanadate concentrations are shown in Figure 2. The data are best approximated by a simple noncompetitive model of inhibition, providing a K_i for vanadate of $4.3 \pm 0.5 \mu\text{M}$. The inhibition is complicated because vanadate can potentially bind at two sites on the dimeric enzyme and may not readily dissociate. However, even with these potential complications, the data are not consistent with a competitive mode of inhibition by vanadate. Therefore, the vanadate inhibition results suggest that P_i release occurs prior to ADP release, in agreement with the ADP inhibition results.

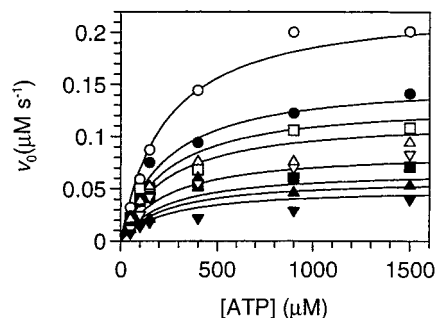


FIGURE 2: Vanadate is a noncompetitive inhibitor of topoisomerase II. Initial velocities were determined from discontinuous ATPase assays in the presence of DNA and eight different ATP concentrations ranging from 50 μM to 1.5 mM. The vanadate concentrations included were 0 (\circ), 2 (\bullet), 3 (\square), 4 (\blacksquare), 7 (\triangle), 10 (\blacktriangle), 12 (∇), and 15 μM (\blacktriangledown). The data are fit to an equation describing simple noncompetitive inhibition: $v_o = [S]V_{\max}/\{K_m(1 + [I]/K_i) + [S](1 + [I]/K_i)\}$. The calculated K_i for vanadate is $4.3 \pm 0.5 \mu\text{M}$.

ATP Hydrolysis Is Sequential. To distinguish between the two reaction pathways shown in Scheme 1, pre-steady-state vanadate inhibition studies were performed. Results of these experiments also provide information on product release. In Figure 3A, pre-steady-state, chemical quench time courses of ATP hydrolysis by topoisomerase II/DNA in the absence (\blacksquare) or presence (\bullet) of 100 μM vanadate are shown. For both time courses, a rapid burst in ADP production is seen. The amplitudes of both bursts are approximately equal to half the enzyme active site concentration; in other words, the burst amplitudes are approximately equal to the dimeric enzyme concentration. The burst rates are also approximately identical. Therefore, vanadate does not perturb the binding or hydrolysis rate of the first ATP, similar to what has been observed in other enzyme systems (11). However, the rate of the steady-state phase decreases with time when vanadate is present. This is consistent with the existence of an enzyme–ADP–vanadate complex.

To determine whether the two ATP are hydrolyzed sequentially or simultaneously, a pulse–chase experiment was also done in the presence of this inhibitor (Figure 3B). For comparison, a chemical quench and a pulse–chase time course performed in the absence of inhibitor are also shown. All three time courses were performed using the same topoisomerase II/DNA preparation. The final ATP active site concentration was 21 μM , indicating that the enzyme dimer concentration was 10.5 μM . From data collected in the absence of vanadate, the burst amplitude in the pulse–chase experiment (19.1 μM) is determined to be approximately twice that observed in the chemical quench experiment (8.9 μM). From the pulse–chase data collected in the presence of 100 μM vanadate, the burst amplitude (8.3 μM) is shown to be approximately equal to half of that seen in a pulse–chase experiment without inhibitor. In other words, in the presence of vanadate the pulse–chase burst amplitude is similar to the chemical quench burst amplitude, suggesting the existence of an enzyme–ATP–ADP complex.

Based upon these steady-state and pre-steady-state inhibition studies, the favored reaction pathway of the two shown in Scheme 1 can be distinguished. As discussed in the preceding paper, in order for the pre-steady-state data to be consistent with simultaneous hydrolysis of both ATP, the rate of ATP hydrolysis must equal the rate of ATP synthesis;

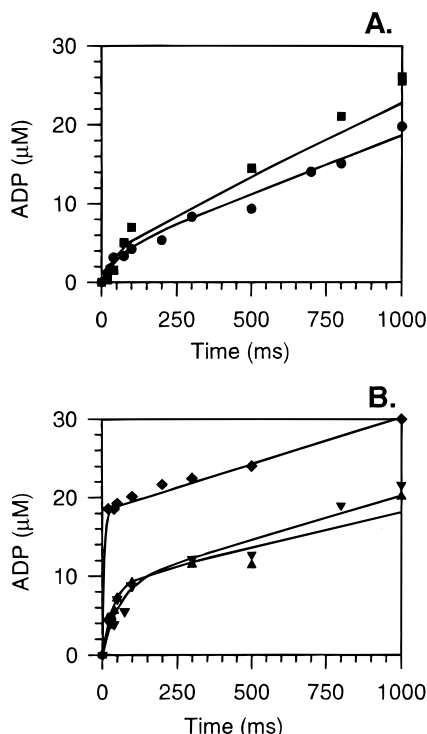


FIGURE 3: Pre-steady-state ATPase assays including vanadate indicate that topoisomerase II sequentially hydrolyzes two ATP. For direct comparison, all data are shown fit to $A(1 - e^{-Bt}) + Ct$. (A) Chemical quench data are shown for assays in which 100 μM vanadate was either absent (\blacksquare) or present (\bullet). The same topoisomerase II/DNA solution that had a measured active site concentration of 9.1 μM was used for the two assays. The values for A , B , and C in the absence of vanadate are $4.0 \pm 0.5 \mu\text{M}$, $20 \pm 5 \text{ s}^{-1}$, and $18 \pm 3 \mu\text{M s}^{-1}$, and in the presence of vanadate are $3.7 \pm 0.4 \mu\text{M}$, $14 \pm 4 \text{ s}^{-1}$, and $14 \pm 2 \mu\text{M s}^{-1}$, respectively. (B) Pulse-chase assays performed in both the absence (\blacklozenge) and presence (\blacktriangledown) of 100 μM vanadate are compared to a chemical quench assay lacking vanadate (\blacktriangledown). All three data sets were obtained using the same topoisomerase II/DNA solution where the total ATP active site concentration was measured as 21 μM . The values for A , B , and C are $8.9 \pm 0.6 \mu\text{M}$, $22 \pm 7 \text{ s}^{-1}$, and $11 \pm 1 \mu\text{M s}^{-1}$ for the chemical quench assay, $19.1 \pm 0.8 \mu\text{M}$, $100 \pm 20 \text{ s}^{-1}$, and $11 \pm 2 \mu\text{M s}^{-1}$ for the standard pulse-chase assay, and $8.3 \pm 0.9 \mu\text{M}$, $22 \pm 5 \text{ s}^{-1}$, and $10 \pm 2 \mu\text{M s}^{-1}$ for the pulse-chase assay including vanadate, respectively.

and either phosphate release must be rate-determining, or it must be fully reversible. The steady-state inhibition studies suggest that the K_i , a reflection of K_d , for P_i is large and that P_i must rapidly dissociate from the enzyme, negating the second constraint for simultaneous hydrolysis. Additionally, if simultaneous ATP hydrolysis occurs and P_i release is not rate-determining, then the burst amplitude for the chemical quench experiment in the presence of vanadate would be equal to the total active site concentration, twice that observed. As rate-determining P_i release is not obviously consistent with the steady-state observations described above, the comparison of burst amplitude data from chemical quench and pulse-chase experiments indicates that topoisomerase II sequentially hydrolyzes the two ATP. A mechanism involving sequential ATP hydrolysis is only consistent with these data if a rate-determining step occurs after hydrolysis of the first ATP, and before products of the second hydrolysis are detected.

The results of the pulse-chase experiment in the presence of vanadate provide further evidence that topoisomerase II

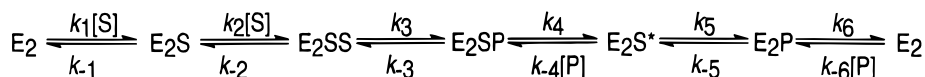
rapidly hydrolyzes one ATP and later in the reaction pathway hydrolyzes the second ATP. If the enzyme hydrolyzes both ATP simultaneously, then the burst amplitude for the pulse-chase experiment performed in the presence of vanadate would be equal to the total active site concentration. This is not observed. The observed results are entirely consistent with sequential hydrolysis where at least P_i from the first ATP hydrolysis is released before hydrolysis of the second ATP.

These results indicate that in the presence of high concentrations of vanadate, topoisomerase II hydrolyzes only one of its two bound ATP. It is predicted that vanadate binds to the enzyme-ADP complex, preventing ADP dissociation. At this point in the reaction cycle, where an enzyme-ADP-vanadate-ATP complex exists, one might predict that turnover should be completely inhibited. The results of the pulse-chase experiment in the presence of vanadate show that only one of the two labeled ATP initially bound to the enzyme is ever hydrolyzed and that residual ATPase activity remains for several seconds. This residual activity suggests that the second labeled ATP must dissociate from the enzyme. This dissociation is not detected in the absence of inhibitor, indicating that the presence of inhibitor alters the preferred reaction pathway.

Products from Hydrolysis of the First ATP Are Released before Hydrolysis of the Second ATP. The pre-steady-state experiments with vanadate suggest a reaction mechanism in which, after topoisomerase II hydrolyzes one ATP, it must release the P_i prior to hydrolyzing the second ATP. The above experiments do not directly address when ADP dissociates from the enzyme. If topoisomerase II releases each product of the first ATP hydrolysis prior to hydrolyzing the second ATP, then in both the pre-steady-state and steady-state time scales the enzyme should have at most one ADP bound. The experimental strategy chosen to determine the number of enzyme-bound ADP entailed having high concentrations of pyruvate kinase and PEP in the reaction to convert any free ADP released from topoisomerase II back to ATP. A similar technique was previously used by Gresser et al. to study the F_1 ATPase (4). It was first necessary to show that under our reaction conditions, pyruvate kinase would convert free ADP back to ATP significantly faster than topoisomerase II would release its ADP. The results of a control chemical quench experiment in which pyruvate kinase and PEP were rapidly mixed with 100 μM [α - ^{32}P]-ADP show that the conversion rate is greater than 2000 $\mu\text{M s}^{-1}$ (data not shown). Therefore, under our standard reaction conditions, pyruvate kinase will very rapidly convert free ADP to ATP.

The results of an experiment using pyruvate kinase and PEP to determine the concentration of ADP bound to topoisomerase II are shown in Figure 4. A chemical quench time course performed in the absence of pyruvate kinase (\bullet) is compared to one performed with the same topoisomerase II/DNA preparation, on the same day, with pyruvate kinase (\blacksquare). The final topoisomerase II dimer concentration was 8.1 μM . In the absence of pyruvate kinase, the chemical quench time course is similar to those previously observed in which the burst amplitude is approximately equal to half the active site concentration ($7.1 \pm 0.8 \mu\text{M}$). When pyruvate kinase is included, a burst in ADP production is again observed with an amplitude of $5.8 \pm 0.6 \mu\text{M}$; however, after

Scheme 2



Scheme 3

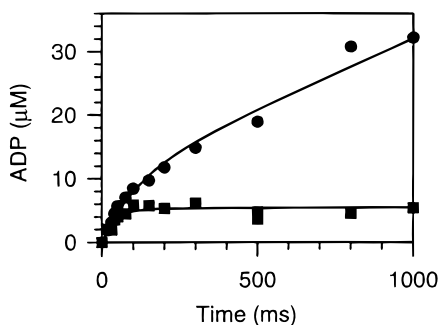
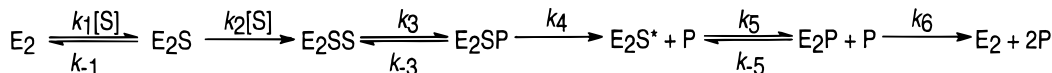


FIGURE 4: A pre-steady-state ADP protection assay using pyruvate kinase and PEP indicates that release of the first ADP contributes to the rate-determining process of ATP hydrolysis by topoisomerase II. Using the same topoisomerase II/DNA solution, a standard chemical quench assay (●) is compared to a chemical quench assay in which 542 units/mL of pyruvate kinase (2.5 mg/mL, final) have been mixed with the labeled ATP solution (■). Both assays contained 8.1 μ M topoisomerase II dimer, 400 μ M ATP, and 10 mM PEP, final concentrations. The data are shown fit to Scheme 3 with the values for rate constants shown in Table 1. The burst amplitudes are 7.1 ± 0.8 and 5.8 ± 0.6 μ M, for the chemical quench and ADP protection data, respectively.

the burst, ADP production plateaus. Under the reaction conditions used, very little of the topoisomerase exists as free enzyme or enzyme bound to two ATP. Therefore, the fact that the concentration of ADP observed in the protection assay never exceeds half the active site concentration suggests that the topoisomerase II dimer is only bound to one ADP at a time. In other words, topoisomerase II is not bound to two ADP at any point in the reaction pathway. The steady-state plateau in ADP production/protection at just below the enzyme dimer concentration indicates that on average, in the steady state, there is approximately one ADP bound to the topoisomerase II dimer. The existence of this steady-state plateau, along with the observed bursts in several different experiments, also indicates that the rate of ADP dissociation must be slow.

The Mechanism for ATP Hydrolysis by Topoisomerase II. The results from experiments presented so far in this and the preceding paper define the chemical and kinetic mechanism for ATP hydrolysis by DNA topoisomerase II. The mechanism that best represents our observations is one in which the enzyme binds two ATP, hydrolyzes one, releases the P_i and ADP produced, hydrolyzes the second ATP, and releases those products. This mechanism can be represented as shown in Scheme 2: where E_2 represents dimeric topoisomerase II bound to DNA, S represents ATP, P represents $ADP \cdot P_i$, and E_2S^* represents a state of topoisomerase II bound to a single ATP that differs from E_2S . Although the results shown in Figures 1 and 2 indicate that P_i is released from the enzyme prior to release of ADP, none of the experiments presented provide direct information on the rate of P_i release. We assume that P_i release from the

enzyme is much faster than ADP release based on the vanadate inhibition studies. Therefore, the two steps of P_i and ADP release have been combined in the steps described by k_4 and k_6 . The results of experiments in this and the preceding paper only address the ATPase reaction pathway; the protein and DNA conformational states associated with each step in the ATPase cycle have not yet been determined. Consequently, the rate constants described in this paper are most likely not microscopic rate constants. Instead, they are probably composite rate constants that include steps of conformational changes as well as the steps of ATP binding and hydrolysis.

The mechanism shown in Scheme 2 can be simplified. Since all of the reactions have been analyzed under initial velocity conditions, insignificant concentrations of product, P, were present. Consequently, $k_{-4}[P]$ and $k_{-6}[P]$ are approximately zero. Studies using the nonhydrolyzable ATP analogue AMPPNP indicate that once this analogue is bound to both ATP active sites, its dissociation rate is extremely slow (J. E. Lindsley, unpublished data). Additionally, the results of the pulse-chase experiments indicate that once two ATP are bound to the enzyme, they are both hydrolyzed before dissociating. Further supporting evidence for k_{-2} being very small comes from experiments attempting to use topoisomerase II to synthesize ATP from ADP and P_i . Results of these experiments indicate that small quantities of ATP can be made, but not released from the enzyme (data not shown). Therefore, k_{-3} and k_{-5} are most likely nonzero, and k_{-2} is insignificant. Based upon this evidence, the mechanism shown in Scheme 2 can be reduced to that shown below in Scheme 3.

In the preceding paper, we concluded that the rate-determining step is after hydrolysis of at least one ATP. For the sequential ATP hydrolysis mechanism to agree with the data, a rate-determining step must occur after the first hydrolysis and before products of the second hydrolysis are detectable. Since a mechanism involving simultaneous ATP hydrolysis is inconsistent with the data presented in this paper, a rate-determining step must occur after hydrolysis of the first ATP, k_3 , and prior to the last step, represented by k_6 . If k_5 were rate-determining, or if $k_{-5} + k_6$ were much larger than k_5 , then E_2S^* would be the most populated enzyme form in the steady state. If this were true, then the signal in the ADP protection experiment would have dropped to zero in the steady state. As the ADP signal in the protection experiment never appreciably dropped below the burst amplitude, k_5 and k_{-5} do not contribute significantly to the rate-determining process. Consequently, the rate-determining process must include k_4 .

Using the method of net rate constants (13), the V_{max} and V_{max}/K_m for topoisomerase II hydrolysis of ATP can now be defined in terms of the rate constants shown in Scheme 3,

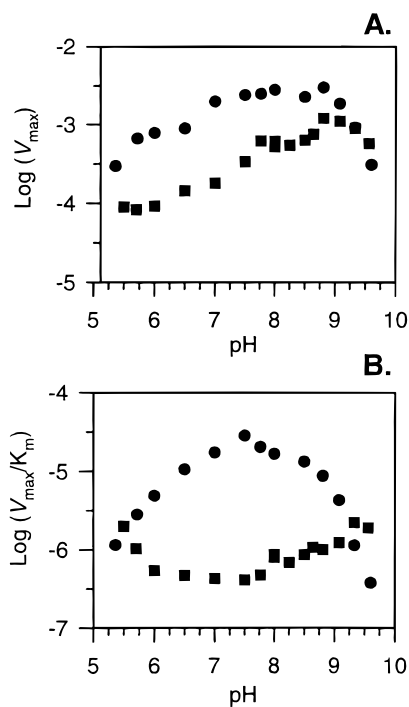


FIGURE 5: pH dependence of the steady-state kinetic parameters V_{\max} (A) and V_{\max}/K_m (B) for ATP hydrolysis by topoisomerase II in the presence (●) and absence (■) of DNA. Values for V_{\max} and V_{\max}/K_m were calculated from initial ATPase velocities at 10 different ATP concentrations. Given the complexity of both the ATPase mechanism and the shapes of these pH–rate profiles, we have not attempted to determine pK_a values from these data.

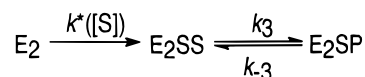
where $[E_{2\text{Tot}}]$ represents the total dimeric enzyme concentration (eqs 1 and 2). These kinetic parameters are derived from a mechanism determined in the presence of DNA. As it appears that topoisomerase II cycles through the same conformational states in the absence and presence of DNA (14), the overall reaction pathway for ATP hydrolysis is most likely the same regardless of the presence of DNA. Therefore, whether DNA is present or absent, the derivations of V_{\max} and V_{\max}/K_m most likely do not change.

$$V_{\max} = \frac{k_3 k_4 k_5 k_6 [E_{2\text{Tot}}]}{k_3 k_4 k_5 + k_3 k_4 k_{-5} + k_3 k_4 k_6 + k_3 k_5 k_6 + k_{-3} k_5 k_6 + k_4 k_5 k_6} \quad (1)$$

$$V_{\max}/K_m = \frac{k_1 k_2 [S] [E_{2\text{Tot}}]}{k_{-1} + (k_1 + k_2) [S]} \quad (2)$$

pH–Rate Profiles. The results of steady-state ATPase experiments can now be interpreted in terms of their effects on different aspects of the reaction mechanism. One example is the steady-state pH–rate profiles of topoisomerase II catalyzed ATP hydrolysis in the presence and the absence of DNA (Figure 5). In both cases, V_{\max} is relatively insensitive to pH, changing at most 10 fold, over a pH range of 5.3–9.6 (Figure 5A). In the absence of DNA, V_{\max}/K_m is also relatively insensitive to pH (Figure 5B). However, in the presence of DNA, V_{\max}/K_m is considerably more pH-sensitive, displaying a bell-shaped curve. In contrast to the similarly shapely V_{\max} pH profiles, the pH profiles for V_{\max}/K_m in the absence and presence of DNA show a dramatic

Scheme 4



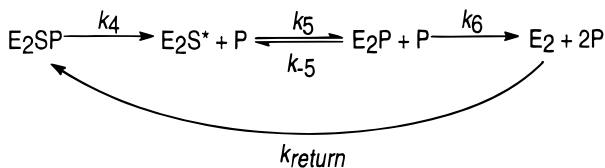
difference. As shown in eq 2, V_{\max}/K_m includes only terms involved in ATP binding. Therefore, when topoisomerase II is bound to DNA, at least one of the steps involved with ATP binding is very pH-sensitive. The difference in V_{\max}/K_m pH data suggests that DNA exerts its largest effect on the binding of ATP to topoisomerase II. In other words, DNA apparently stimulates the rate of ATP hydrolysis by topoisomerase II primarily by increasing the rates of ATP binding. This does not exclude the possibility that DNA also affects the rates of other steps in the reaction pathway.

Determination of Rate Constants. Given that there are nine rate constants for the topoisomerase II mechanism as shown in Scheme 3, the five differential equations describing this mechanism contain nine unknown parameters (note: all details for this section are described in the Appendix). In a single-substrate system, pre-steady-state data can detect individual enzyme intermediates (15). However, for a two-substrate system such as topoisomerase II, the data can only resolve combinations of enzyme complexes. Consequently, fitting the data to Scheme 3 in order to determine the rate constants cannot be done with confidence simply by using a numerical integration program. Utilization of such a program provides many different solutions to these equations that all appear to be good fits to the data. Without reasonable initial estimates for each of the nine rate constants, it is not possible to distinguish which of these solutions is correct. To estimate the rate constants, the pre-steady-state data, obtained when the substrate concentration was near saturation, were analyzed by separating the reaction mechanism into three components: ATP binding, the fast phase, and the slow phase. Since the burst rate exceeds the steady-state rate by greater than 10-fold, the pre-steady-state data can be divided into a fast and a slow phase based upon the identification of the first rate-determining step. To separately examine the complex binding nature of the two ATP, the fast phase was further divided into binding of the two ATP and hydrolysis of the first ATP. The slow phase of the reaction includes the transition from the fast phase to steady state, as well as the steady state itself. As the first rate-determining step is represented by k_4 , the fast phase includes $k_1[S]$, k_{-1} , $k_2[S]$, k_3 , and k_{-3} , and the slow phase includes k_4 , k_5 , k_{-5} , and k_6 .

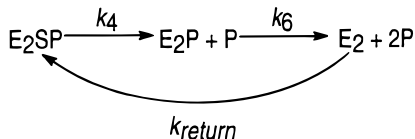
The binding phase of the mechanism includes $k_1[S]$, k_{-1} , and $k_2[S]$. The level of positive cooperativity in ATP binding (7) and the assumption that k_{-2} is negligible indicate that $k_{-1} + k_2[S] \gg k_1[S]$. Based upon the solutions to the differential equations for the enzyme states involved in ATP binding, an effective net rate binding constant, $k^*(S)$, can be defined, where $k^*(S) = k_1[S] \{k_2[S] / (k_2[S] + k_{-1}[S])\}$. When the substrate concentration is large, $k^*(S)$ reduces to $k_1[S]$; at lower substrate concentrations, the binding rate is reduced by k_{-1} .

When examining only the fast phase of the mechanism involving binding and hydrolysis of the first ATP, Scheme 3 can now be reduced to Scheme 4.

Scheme 5



Scheme 6



The fast phase can be examined under two different conditions, when substrate is either saturating or subsaturating. When the substrate concentration is large enough to ensure saturation of the enzyme, the burst rate of both the chemical quench and the pulse–chase experiments will be dependent upon k_3 and $k_1[\text{S}]$, respectively. Substrate binding can be described solely by $k_1[\text{S}]$. In other words, free enzyme will go to E_2SS at a rate equal to $k_1[\text{S}]$. In the fast phase, the observed data for the chemical quench experiment reflects the formation of the E_2SP complex. The observed data for the pulse–chase experiment reflect $2(\text{E}_2\text{SS} + \text{E}_2\text{SP})$; the factor of 2 is required because each E_2SS and E_2SP complex generates two products. The solutions for the differential equations describing E_2SP and E_2SS show that the burst rate for the chemical quench is dependent upon k_3 , while the burst rate for the pulse–chase reflects $k_1[\text{S}]$. As the pulse–chase burst rate is at least 2-fold faster than the chemical quench burst rate, the rate of binding, $k_1[\text{S}]$, is greater than the rate of ATP hydrolysis, k_3 . When the substrate concentration is subsaturating, $k^*(\text{S})$ becomes rate-determining, such that $k^*(\text{S})$ is less than k_3 , and the formation of E_2SP is controlled by $k^*(\text{S})$.

The slow phase of the reaction can be described by a reduced form of Scheme 3, in which all steps following and including the rate-determining step are shown in Scheme 5.

The rate constant k_{return} includes all steps found in the fast phase of the reaction, and therefore, as long as the substrate concentration is saturating, does not contribute to the slow phase. If a fast step occurs between two slower steps, the data will only reflect the slower processes, obscuring the fast one. Based on the rapid hydrolysis of the first ATP, followed by its slower product release, we make the assumption that hydrolysis of the second ATP is faster than its product release. This assumption leads to the following simplified mechanism, shown in Scheme 6.

At the beginning of the slow phase, immediately following the burst, the majority of the enzyme is in the E_2SP form. Once steady state has been established, the majority of the enzyme is in either the E_2SP or the E_2P form. In the transition between the fast and slow phases, the concentration of enzyme in the E_2SP form becomes distributed into E_2SP and E_2P forms. The solutions for the differential equations describing E_2SP and E_2P predict that there will be a pause in product formation immediately after the burst in pulse–chase experimental data. The steady-state rate of product formation provides estimates for $(k_4k_6/k_4 + k_6)$ as described by the differential equations for E_2SP and E_2P .

Table 1: Rate Constants for ATP Hydrolysis by DNA Topoisomerase II^a

$\text{E}_2 + \text{S} \rightleftharpoons \text{E}_2\text{S}$	k_1 ($\mu\text{M s}^{-1}$)	0.3 ^{b,c}
	k_{-1} (s^{-1})	1000
$\text{E}_2\text{S} + \text{S} \rightarrow \text{E}_2\text{SS}$	k_2 ($\mu\text{M s}^{-1}$)	3
$\text{E}_2\text{SS} \rightleftharpoons \text{E}_2\text{SP}$	k_3 (s^{-1})	40–50 ^d
	k_{-3} (s^{-1})	≤ 4
$\text{E}_2\text{SP} \rightarrow \text{E}_2\text{S}^* + \text{P}$	k_4 (s^{-1})	3–5
$\text{E}_2\text{S}^* \rightleftharpoons \text{E}_2\text{P}$	k_5 (s^{-1})	40–50
	k_{-5} (s^{-1})	≤ 4
$\text{E}_2\text{P} \rightarrow \text{E}_2 + \text{P}$	k_6 (s^{-1})	2–7

^a All reactions were performed at 25 °C in 1 × reaction buffer. ^b Rate constants were initially estimated using singular perturbation theory and then optimized against χ^2 using a numerical program. ^c Values for k_1 , k_{-1} , and k_2 were determined based upon our fits to $k^*(\text{S})$. $k^*(\text{S})$ varies as described in Figure 6C. ^d Ranges for rate constants are shown as data from different experiments are sensitive to different parameter combinations.

Based upon these techniques of kinetic parameter estimation, values for all nine rate constants were obtained for the mechanism shown in Scheme 3. These values were then entered into a minimization program that fit 16 pre-steady-state data sets to the mechanism, increasing the precision of the reported rate constants (Table 1). These data sets included 1 ADP protection assay, 4 pulse–chase assays, and 11 chemical quench assays, at various ATP concentrations.

Although a qualitative analysis of these pre-steady-state data has provided many new insights into the ATPase reaction mechanism of topoisomerase II, the quantitative analysis provides further insights. A comparison between two sets of pulse–chase and chemical quench results, one performed at subsaturating ATP (100 μM) and the other at saturating ATP (350 μM), is shown in Figure 6A,B, respectively. As described above, if the ATP concentration is saturating, the burst amplitude and burst rate for the pulse–chase experiment are twice those of the chemical quench. When ATP is subsaturating, a 10% increase in the burst amplitude and essentially no change in the burst rate are observed when comparing the pulse–chase to the chemical quench results. These results support the hypothesis that over a small range of ATP concentrations, the binding dynamics of topoisomerase II change greatly. At 100 μM ATP, two processes, ATP binding and ADP dissociation, are both rate-determining. At ATP concentrations below 100 μM , ATP binding is the rate-determining step. Models of ATP binding rates as functions of cooperativity are shown in Figure 6C, clearly showing that binding rates are nonlinear with ATP concentration. The level of positive cooperativity is shown as a , where $a = k_2/k_1$. For a burst in ADP production to be observed, binding must be faster than the rate-determining process, as indicated by the dashed line. This threshold is drawn to indicate the value for k_{cat} of ATP hydrolysis by topoisomerase II. Our data are fit with $a = 10$. At this level of cooperativity, this model shows that a burst in ADP production is expected for ATP concentrations greater than 100 μM , as is clearly seen in the preceding paper. When ATP is saturating, the two product release steps, k_4 and k_6 , solely contribute to rate-determination of the reaction cycle. To better understand the relative magnitude of k_4 to k_6 , models of both chemical quench and pulse–chase time courses are shown for various $k_4:k_6$ ratios (Figure 6D). Although our data may not distinguish some of the subtleties

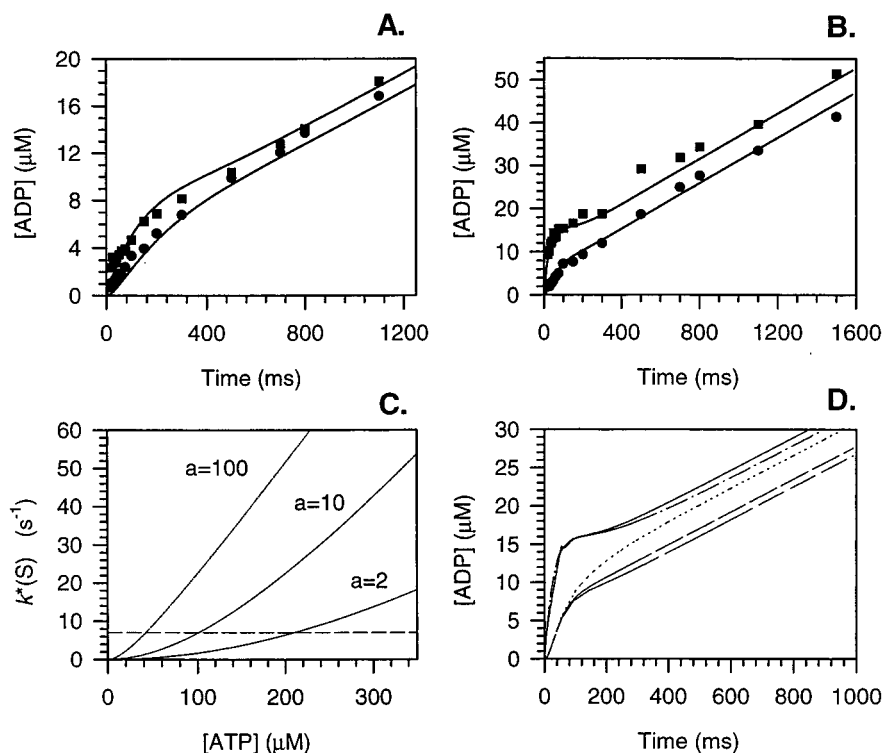


FIGURE 6: Modeling the mechanism for ATP hydrolysis by topoisomerase II. Chemical quench (●) and pulse-chase (■) results are shown for assays performed at 100 μM ATP (A) and 350 μM ATP (B). In each experiment, the same topoisomerase II/DNA solution was used, where the total ATP active site concentration was 13.4 μM . All four data sets are shown fit to Scheme 3 with the values for rate constants given in Table 1. In panel C, the binding function $k^*(S)$ is modeled as a function of substrate concentration at three different levels of positive cooperativity in binding, represented by the factor a , where $a = k_2/k_1$. The dashed line is drawn at the rate equal to k_{cat} for ATP hydrolysis by topoisomerase II. Only when $k^*(S)$ appreciably exceeds this rate will a burst in ADP production be detectable. In panel D, models of both pulse-chase and chemical quench data are shown as functions of time, based on Scheme 3. The values of k_4 and k_6 , describing the two steps contributing to the rate-determining process, are altered in these models. For models of chemical quench data, $k_4 = 7.0 \text{ s}^{-1}$ and $k_6 = 1.9 \text{ s}^{-1}$ (—); $k_4 = k_6 = 3.0 \text{ s}^{-1}$ (- -); $k_4 = 1.9 \text{ s}^{-1}$ and $k_6 = 7.0 \text{ s}^{-1}$ (···). For the pulse-chase models, $k_4 = k_6 = 3.0 \text{ s}^{-1}$ (- · -); $k_4 = 7.0 \text{ s}^{-1}$ and $k_6 = 1.9 \text{ s}^{-1}$, as well as $k_4 = 1.9 \text{ s}^{-1}$ and $k_6 = 7.0 \text{ s}^{-1}$ (—). In these models, the total enzyme concentration, $E_{2,\text{Tot}}$, is set at 8.0 μM , and $k^*(S)$, k_3 , and k_5 are each set at 40 s^{-1} . As k_{-3} and k_{-5} do not significantly contribute to the overall reaction dynamics, these rate constants have been ignored.

between these models, k_6 is of the same order of magnitude as k_4 . The pulse-chase model also indicates that a pause in ADP production should be observed immediately after the burst and before steady-state ADP production. In fact, any enzyme mechanism displaying burst kinetics and having two rate-determining steps should theoretically also display a similar pause. Although the pulse-chase data for topoisomerase II are consistent with the existence of such a pause (Figure 6B), there are not enough data points to definitively show the pause.

DISCUSSION

DNA topoisomerase II has an unexpected and complex mechanism for ATP hydrolysis. Our findings suggest that after binding two ATP, the enzyme stochastically hydrolyzes one and releases those products before hydrolyzing the second ATP. Following the first ATP hydrolysis, at least one slow step in the mechanism occurs before products of the second ATP hydrolysis can be detected. The sequential hydrolysis of ATP and product release steps indicate that the mechanism for topoisomerase II is considerably more complicated than previously depicted. This new mechanism, shown in Scheme 3, predicts transient asymmetry to occur within an enzyme reaction cycle that has always been thought of as symmetric.

The results of chemical quench and pulse-chase experiments described in the preceding paper could be explained by two general reaction pathways, as shown in Scheme 1. The burst in ADP production observed in chemical quench experiments indicates that at least one ATP is rapidly hydrolyzed, prior to a rate-determining step. The doubling of the burst amplitude in pulse-chase experiments compared to the bursts in chemical quench experiments suggests that two ATP are bound to the enzyme and both are hydrolyzed before additional ATP binds. For these results to be consistent with the simultaneous hydrolysis mechanism shown as the lower pathway of Scheme 1, the rates of ATP hydrolysis and synthesis must be equal. Additionally, either the release of the first product of hydrolysis must be rate-determining or product release must be completely reversible. In contrast, for these results to be consistent with a sequential hydrolysis mechanism, only one constraint must be imposed: the rate-determining step must occur between hydrolysis of the first ATP and detection of products of the second hydrolysis.

The results described in this paper clearly indicate which of these two potential pathways most accurately reflects the general ATPase mechanism of topoisomerase II. Results from inhibition studies are not consistent with a simultaneous hydrolysis mechanism. These studies indicate that P_i is

released rapidly, prior to ADP. Given that the P_i concentration is negligible under our reaction conditions and the K_d for P_i is most likely very large, P_i release is essentially irreversible. Consequently, the constraints necessary for simultaneous hydrolysis appear to be invalid. Additionally, using pre-steady-state kinetics, we have been able to identify individual enzyme intermediates that exist along the reaction pathway. Chemical quench and pulse-chase experiments performed in the presence of vanadate show the existence of an enzyme-ATP-ADP intermediate, and not an enzyme-ADP-ADP intermediate, consistent only with the sequential hydrolysis mechanism.

Together, these results indicate that topoisomerase II hydrolyzes two ATP sequentially and suggest that the products of the first hydrolysis are released before the second ATP is hydrolyzed. Based upon the results of pre-steady-state inhibition studies, at least the P_i , and most likely the ADP, from the first ATP hydrolysis must be released before the second ATP is hydrolyzed. Results from the ADP protection assay indicate that the first ADP is also released prior to hydrolysis of the second ATP. Additionally, these results show that release of the first ADP contributes to the rate-determining process.

The combination of results from all of these experiments identified the intermediates of the topoisomerase II ATPase pathway, as shown in Scheme 3. Based upon rate constant determination, two steps were shown to contribute to the rate-determining process, k_4 and k_6 . This is in agreement with what has previously been predicted for DNA gyrase (16), namely, that the rate-determining step for ATP hydrolysis is release of $ADP \cdot P_i$. These steps are most likely coupled to conformational changes, and we speculate that release of the first products is also coupled to DNA transport.

Without DNA, topoisomerase II slowly hydrolyzes ATP. Based on previous studies, it appears that the enzyme cycles through the same conformational states in both the absence and presence of DNA (14). Therefore, we assume that Scheme 3 describes the ATPase reaction pathway of topoisomerase II when DNA is both present and absent. However, some or all of the individual rate constants are different. To begin to understand the coupling between ATPase activity and the enzyme-DNA interactions, effects of DNA on the ATPase reaction mechanism were analyzed using both pre-steady-state and steady-state techniques. As shown in the preceding paper, without DNA there is no indication of a burst in ADP production by topoisomerase II, suggesting that ATP binding or hydrolysis is rate-determining. Consequently, the rates associated with at least one of these processes are greatly stimulated by DNA. Analysis of steady-state pH-rate profiles suggests that DNA stimulates the rates of ATP binding more than rates describing other steps of the ATPase reaction. The DNA stimulation of ATP binding was previously suggested from results of experiments with DNA gyrase (17). This is reasonable when considering the efficiency of DNA transport by topoisomerase II. Once ATP is bound, the enzyme is no longer in a conformation that can bind DNA (14). Therefore, if in the absence of bound DNA, ATP binds slowly, the enzyme will remain for longer periods of time in a conformation favoring DNA capture.

Although each pre-steady state experiment contains an enormous amount of quantitative information, extracting this

information is nontrivial. Values for the nine rate constants had to be obtained in order to fit the data to the mechanism shown in Scheme 3. It was not possible to reduce the number of unknown rate constants by fitting the data to a simplified mechanism in which either the two ATP bind simultaneously or the ATP active sites act independently. Likewise, it was not possible to use equilibrium constants or steady-state parameters other than k_{cat} and k_{cat}/K_m , to reduce the number of unknown rate constants. Knowledge of the K_d for ATP would have reduced the number of unknowns; however, determination of this K_d was not possible due to the complexities of cooperative binding, hydrolysis of the substrate, and essentially irreversible binding of nonhydrolyzable analogues. It was noted that individual rate constants are particularly sensitive to data from different types of pre-steady-state experiments (Appendix). Based on this sensitivity, estimates for all nine rate constants were obtained. All of the pre-steady-state data shown in this paper were fit to Scheme 3 with the values for rate constants shown in Table 1. One benefit of fitting the data in this way was the identification of a pause in ADP production that is predicted to occur immediately after the pulse-chase burst. The length of the pause indicates the ratio involving k_4 and k_6 , the two steps that determine the steady-state rate.

Three assumptions were made in order to fit the data; none of these assumptions affect the proposed mechanism, but only the values of particular rate constants. The first assumption is that topoisomerase II binds the second ATP with at least a 10-fold greater affinity than it binds the first ATP. This assumption is supported by analysis of steady-state and pre-steady-state ATPase assays, as well as conformational studies of topoisomerase II. If this assumption is incorrect and the enzyme binds the two ATP with nearly equal affinity, then the values for k_1 , k_{-1} , and k_2 will differ from those given in Table 1. The next assumption is that binding of the second ATP is essentially irreversible. Several types of experiments indicate that once nonhydrolyzable ATP analogues are bound to either topoisomerase II (J.E.L., unpublished data) or gyrase (17), they do not readily dissociate. The results of these experiments have been interpreted to indicate that once two ATP are bound, the enzyme is in a conformational state that cannot readily release ATP. Additionally, a burst amplitude equal to the ATP active site concentration in the pulse-chase experiments could only be obtained if binding the two ATP is essentially irreversible. If this assumption is incorrect and k_{-2} is not negligible, then the values for k_2 and k_3 given in Table 1 would be underestimates of the true values. Additionally, the interpretation of DNA stimulation from the pH-rate profiles would need to be altered to include ATP hydrolysis, as V_{max}/K_m would now include k_3 . The last assumption is that the rate of hydrolysis of the second ATP, described by k_5 , is faster than its product release, k_6 . This assumption is based upon mechanistic symmetry and the fact that the first ATP hydrolysis, k_3 , is faster than its product release, k_4 . Based upon modeling the mechanism, the rate constants k_5 and k_6 cannot be equal. Therefore, if this last assumption is wrong, then the values for k_5 and k_6 will essentially be swapped.

Under our reaction conditions, the most favored pathway for ATP hydrolysis by topoisomerase II is described by Scheme 3. However, it may be possible that the enzyme

each of the three sites cycles between different conformations, with no two ever being in the same state (32). A hexameric helicase has been proposed to have a similar mechanism (33). Additionally, the two heads of kinesin (34, 35) and the two protomers of the dimeric rep helicase (33) are also thought to be in different states relative to nucleotide binding; when one active site has ATP bound, the other either is free or has ADP bound. These different enzyme–nucleotide states are thought to direct altered interactions with the cosubstrates, microtubules or DNA, respectively. In contrast, topoisomerase II initiates its reaction cycle by binding two ATP with positive cooperativity. Sequential hydrolysis then follows, indicating that the two halves of the enzyme are in different nucleotide-bound states for much of the enzyme's reaction cycle. One unexpected feature of this mechanism is the prediction that the topoisomerase II dimer will not remain entirely symmetric throughout its cycle. Each crystal structure of a dimeric type II topoisomerase fragment shows *C2* symmetry (21, 36, 37). Symmetry must remain in the vicinity of the active site tyrosines in order to have coordinated DNA cleavage and separation of the cleaved strands to allow transport of the second DNA segment. Although dimeric topoisomerase II may be asymmetric with respect to the nucleotides bound, the overall conformational state of the enzyme may remain symmetric. In support of this idea, a topoisomerase II dimer constructed to bind only one ATP maintains overall symmetry in the presence of a nonhydrolyzable ATP analogue (38). In light of these results, it will be particularly interesting to analyze the conformation of the enzyme bound to one ATP and one ADP. This mechanism also suggests that the two ATP may be hydrolyzed by DNA topoisomerase II for different functions.

ACKNOWLEDGMENT

We thank Drs. J. P. Keener and J. Mathis for helpful discussions.

APPENDIX

Based upon the different phases observed in the pre-steady-state ATPase data, the mechanism shown in Scheme 3 was separated into subsystems involving different time scales, the fast phase and slow phase. This method allows analytical solutions to be derived for the different phases of the data and therefore allows observed data to be correlated to a specific portion of the reaction mechanism that can be described by a limited number of rate constants. The error associated with these estimates is proportional to the size of the ratio of the different time scales used to separate the mechanism. Once estimates are obtained, numerical analysis is performed to increase the precision of the values for the rate constants, i.e., minimize the χ^2 error. The following results can all be rigorously derived using singular perturbation theory (8); however, for conciseness only the essence of the arguments is presented. In all of the following derivations, it is assumed that the concentration of substrate remains essentially unchanged, $d[S]/dt \approx 0$. This assumption is valid for all of the data analyzed.

Binding Dynamics. Based upon the assumptions outlined in the paper, a set of differential equations for enzyme complexes involved with substrate binding are shown below.

$$\frac{d}{dt}[E_2] = k_6[E_2P] - k_1[S][E_2] + k_{-1}[E_2S]$$

$$\frac{d}{dt}[E_2S] = k_1[S][E_2] - (k_2[S] + k_{-1})[E_2S]$$

$$\frac{d}{dt}[E_2SS] = k_2[S][E_2S] - k_3[E_2SS] + k_{-3}[E_2SP]$$

By nondimensionalizing time in the above set of differential equations by setting $\tau = k_1[S]t$, we obtain

$$\frac{d}{d\tau}[E_2] = \frac{k_6}{k_1[S]}[E_2P] - [E_2] + \frac{k_{-1}}{k_1[S]}[E_2S]$$

$$\frac{d}{d\tau}[E_2S] = [E_2] - \frac{1}{\epsilon}[E_2S]$$

$$\frac{d}{d\tau}[E_2SS] = \frac{k_2[S]}{k_1[S]}[E_2S] - \frac{k_3}{k_1[S]}[E_2SS] + \frac{k_{-3}}{k_1[S]}[E_2SP]$$

where $\epsilon = k_1[S]/(k_2[S] + k_{-1})$. The value for ϵ is small since $k_2[S] + k_{-1} \gg k_1[S]$, as expected for positive cooperativity in substrate binding. In this section, there is no need to make assumptions about the size of other coefficients in the above system.

The differential equation for $[E_2S]$ shows that the concentration of E_2S is small, i.e., of the order ϵ or smaller. This requires us to rescale $[E_2S]$ to $\epsilon[E_2S_1]$; i.e., $[E_2S] = \epsilon[E_2S_1]$. By substituting $\epsilon[E_2S_1]$ into the differential equations for $[E_2S]$ and setting the small parameter ϵ to zero, we find that $[E_2S_1] = [E_2]$ (i.e., [free E_2]) and thus $[E_2S] = \epsilon[E_2]$. Substituting this solution for $[E_2S]$ into the differential equations for $[E_2]$ and $[E_2SS]$, and rescaling to the original time scale (t), two new differential equations are derived that do not contain $[E_2S]$.

$$\frac{d}{dt}[E_2] = k_6[E_2P] - k^*([S])[E_2]$$

$$\frac{d}{dt}[E_2SS] = k^*([S])[E_2] - k_3[E_2SS] + k_{-3}[E_2SP]$$

This reduced system of differential equations represents the mass action laws for a scheme similar to Scheme 4. In these equations, the effective binding rate constant $k^*([S])$ has been introduced, where $k^*([S]) = k_1[S] - \{k_2[S]/(k_2[S] + k_{-1})\}$.

Fast Phase Dynamics. The differential equations describing the fast phase or burst subsystem shown in Scheme 4 are

$$\frac{d}{dt}[E_2] = -k^*([S])[E_2]$$

$$\frac{d}{dt}[E_2SS] = k^*([S])[E_2] - k_3[E_2SS] + k_{-3}[E_2SP]$$

$$\frac{d}{dt}[E_2SP] = k_3[E_2SS] - k_{-3}[E_2SP]$$

This subsystem can be reduced to two differential equations by using the conservation equation of $[E_{2, \text{Tot}}] = [E_2] + [E_2SS] + [E_2SP]$. When the concentration of ATP is very large, such that $k^*([S]) \gg k_3, k_{-3}$, Scheme 4 can be separated into

extremely rapid binding and slower formation of $[E_2SP]$. Equations for binding are obtained by setting k_3 and k_{-3} to zero, since they are small relative to $k^*(S)$. These equations can then be solved using the initial conditions that $[E_2]_{t=0} = [E_{2,Tot}]$ and $[E_2SS]_{t=0} = [E_2SP]_{t=0} = 0$ to obtain the following solutions:

$$[E_2] = [E_{2,Tot}]e^{-k^*(S)t}$$

$$[E_2SS] = [E_{2,Tot}]\{1 - e^{-k^*(S)t}\}$$

where $[E_2SP]$ remains zero. As expected, almost all free enzyme, E_2 , is rapidly converted into E_2SS , and since binding is effectively irreversible, the conservation condition for the remainder of the burst dynamics is

$$[E_{2,Tot}] = [E_2SS] + [E_2SP]$$

Hydrolysis to form E_2SP is shown as the last step in Scheme 4. Using the conservation equation shown above, this is completely modeled by

$$\frac{d}{dt}[E_2SP] = k_3([E_{2,Tot}] - [E_2SP]) - k_3[E_2SP]$$

which can be solved with $[E_2SP]_{t=0} = 0$ to produce

$$[E_2SP] = \frac{k_3}{k_3 + k_{-3}}[E_{2,Tot}]\{1 - e^{-(k_3+k_{-3})t}\}$$

$$[E_2SS] = [E_{2,Tot}] - \frac{k_3}{k_3 + k_{-3}}[E_{2,Tot}]\{1 - e^{-(k_3+k_{-3})t}\}$$

The complete solution can be written by using the appropriate matching conditions for fast binding and slower hydrolysis:

$$[E_2] = [E_{2,Tot}]e^{-k^*(S)t}$$

$$[E_2SS] = [E_{2,Tot}]\{1 - e^{-k^*(S)t}\} - \frac{k_3}{k_3 + k_{-3}}[E_{2,Tot}]\{1 - e^{-(k_3+k_{-3})t}\}$$

$$[E_2SP] = \frac{k_3}{k_3 + k_{-3}}[E_{2,Tot}]\{1 - e^{-(k_3+k_{-3})t}\}$$

The chemical quench and ADP protection assay signals are both equal to the level of $[E_2SP]$, which is described above. The signal from the pulse–chase assays equals $2([E_2SP] + [E_2SS])$, which in turn equals $2[E_{2,Tot}]\{1 - e^{-k^*(S)t}\}$. Note that since the burst amplitudes of pulse–chase and chemical quench assays are approximately equal to $[E_{2,Tot}]$ and $2[E_{2,Tot}]$, respectively, it must be that $k_3 \gg k_{-3}$.

When the binding rate is of the same order as the rate for hydrolysis, $k^*(S) \approx k_3$. Although we can solve the subsystem described by Scheme 4 in general, the dependence of the solutions on the rate constants is not of a simple functional form. However, because effectively k_{-3} approximately equals zero, the k_{-3} terms can be ignored, and the three differential equations of this subsystem can be solved sequentially to obtain

$$[E_2] = [E_{2,Tot}]e^{-k^*(S)t}$$

$$[E_2SS] = [E_{2,Tot}]\frac{k^*(S)}{k^*(S) - k_3}\{e^{-k_3t} - e^{-k^*(S)t}\}$$

$$[E_2SP] = [E_{2,Tot}]\left\{1 - \frac{k^*(S)e^{-k_3t} - k_3e^{-k^*(S)t}}{k^*(S) - k_3}\right\}$$

Again, the chemical quench and ADP protection signals are described by the change in $[E_2SP]$ with time. The pulse–chase signal remains as described above. Note that as $k^*(S)$ decreases, the chemical quench signal, $[E_2SP]$, approaches the shape described by a single-exponential function $[E_{2,Tot}]\{1 - e^{-k^*(S)t}\}$. If $k^*(S) \ll k_3$, then $k^*(S)$ approximately equals k_4 , and thus no substantial burst will be observed.

Slow Phase Dynamics: Post Burst. Here we assume that the rates involved in the second hydrolysis step and the second product release are the same order of magnitude as the corresponding rates of the first hydrolysis and product release. Thus, when the concentration of substrate is large, binding and both hydrolysis steps can be taken to be in quasi-equilibrium after formation of the initial burst, as their associated rate constants are much larger than those describing product release. This results in reaction Scheme 6, as described in the body of the paper. The governing system of differential equations for this scheme is

$$\frac{d}{dt}[E_2SP] = -k_4[E_2SP] + k_6[E_2P]$$

$$\frac{d}{dt}[E_2P] = k_4[E_2SP] - k_6[E_2P]$$

The conservation condition, $[E_{2,Tot}] = [E_2SP] + [E_2P]$, lets this system be reduced to a linear first-order differential equation for $[E_2P]$:

$$\frac{d}{dt}[E_2P] = k_4[E_{2,Tot}] - (k_4 + k_6)[E_2P]$$

This equation can be solved with $[E_2P]_{t=0} = 0$ to obtain the solutions for $[E_2P]$ and $[E_2SP]$:

$$[E_2P] = \frac{k_4}{k_4 + k_6}[E_{2,Tot}]\{1 - e^{-(k_4+k_6)t}\}$$

$$[E_2SP] = [E_{2,Tot}] - \frac{k_4}{k_4 + k_6}[E_{2,Tot}]\{1 - e^{-(k_4+k_6)t}\}$$

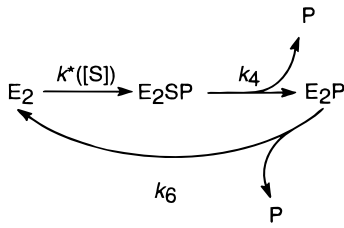
The equation for product concentration, $[P]$, is

$$\frac{d}{dt}[P] = k_4[E_2SP] + k_6[E_2P]$$

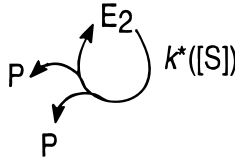
By substituting the solutions for $[E_2SP]$ and $[E_2P]$ into the above equation and integrating with $[P]_{t=0} = 0$, we are able to solve for $[P]$:

$$[P] = [E_{2,Tot}]\left\{\left(\frac{2k_4k_6}{k_4 + k_6}\right)t + \frac{k_4(k_4 - k_6)}{(k_4 + k_6)^2}\{1 - e^{-(k_4+k_6)t}\}\right\}$$

Scheme 8



Scheme 9



The modeled results of the post-burst experimental signals would therefore be the following:

$$\text{chemical quench signal} = [\text{E}_2\text{SP}] + [\text{E}_2\text{P}] + [\text{P}]$$

$$= [\text{E}_{2,\text{Tot}}] + \frac{2k_4k_6}{k_4 + k_6}[\text{E}_{2,\text{Tot}}]t + [\text{E}_{2,\text{Tot}}] \frac{k_4(k_4 - k_6)}{(k_4 + k_6)^2} \{1 - e^{-(k_4+k_6)t}\}$$

$$\text{ADP protection signal} = [\text{E}_2\text{SP}] + [\text{E}_2\text{P}] = [\text{E}_{2,\text{Tot}}]$$

$$\text{pulse-chase signal} = 2[\text{E}_2\text{SP}] + [\text{E}_2\text{P}] + [\text{P}] =$$

$$[\text{E}_{2,\text{Tot}}] + [\text{E}_2\text{SP}] + [\text{P}] = 2[\text{E}_{2,\text{Tot}}] + \frac{2k_4k_6}{k_4 + k_6}[\text{E}_{2,\text{Tot}}]t - [\text{E}_{2,\text{Tot}}] \frac{2k_4k_6}{(k_4 + k_6)^2} \{1 - e^{-(k_4+k_6)t}\}$$

The last term in the pulse-chase signal characterizes the “pause” as an exponential decay away from a simple linear increase in product formation, as seen in Figure 6D. Likewise, either a smaller pause or an increase in ADP production could be observed in the chemical quench data based upon the relative magnitudes of k_4 and k_6 .

When Substrate Concentrations Are Small. When substrate concentrations are low, binding is slow and therefore there is little or no burst phase, and slow dynamics dominate throughout the reaction. Under these conditions, those steps representing hydrolysis are much faster than any other part of the reaction. Consequently, the steps involved in hydrolysis can be taken to be in quasi-equilibrium. The resulting mechanism is shown in Scheme 8. By using the conservation of mass equation $[\text{E}_{2,\text{Tot}}] = [\text{E}_2] + [\text{E}_2\text{SP}] + [\text{E}_2\text{P}]$, the system of differential equations describing this reaction can be written as

$$\frac{d}{dt}[\text{E}_2\text{SP}] = k^*([\text{S}])([\text{E}_{2,\text{Tot}}] - [\text{E}_2\text{SP}] - [\text{E}_2\text{P}]) - k_4[\text{E}_2\text{SP}]$$

$$\frac{d}{dt}[\text{E}_2\text{P}] = k_4[\text{E}_2\text{SP}] - k_6[\text{E}_2\text{P}]$$

This nonhomogeneous second-order linear system can be solved analytically; however, the solutions are complex, involving combinations of the parameters (not shown). However, since high substrate concentration data have given estimates for k_4 and k_6 , the sole remaining unknown parameter that exists is $k^*([\text{S}])$. $k^*([\text{S}])$ can be estimated by minimizing the χ^2 error when the data are fit to the analytical solutions.

If the substrate concentrations are very low, so that $k^*([\text{S}]) \ll k_4, k_6$, then $k^*([\text{S}])$ is the sole rate-determining step and the binding of substrate will dominate the overall reaction. Thus, at any time, almost all of the free enzyme is in the free state, $[\text{E}_2] \sim [\text{E}_{2,\text{Tot}}]$, and only an equation for $[\text{P}]$ is needed to describe the full reaction (Scheme 9):

$$\frac{d[\text{P}]}{dt} = 2k^*([\text{S}])[\text{E}_{2,\text{Tot}}]t$$

Therefore,

$$[\text{P}] = 2k^*([\text{S}])[\text{E}_{2,\text{Tot}}]t$$

Note that the chemical quench signal = pulse-chase signal = $[\text{P}]$ are slow, linearly increasing signals, whereas the ADP protection signal is approximately zero.

REFERENCES

- Berger, J. M., and Wang, J. C. (1996) *Curr. Opin. Struct. Biol.* 6, 84–90.
- Wang, J. C. (1996) *Annu. Rev. Biochem.* 65, 635–692.
- Ha, J., and McKay, D. B. (1994) *Biochemistry* 33, 14625–14635.
- Gresser, M. J., Myers, J. A., and Boyer, P. D. (1982) *J. Biol. Chem.* 257, 12030–12038.
- Ellis, K. J., and Morrison, J. F. (1982) *Methods Enzymol.* 87, 405–426.
- Worland, S. T., and Wang, J. C. (1989) *J. Biol. Chem.* 264, 4412–4416.
- Lindsay, J. E., and Wang, J. C. (1993) *J. Biol. Chem.* 268, 8096–8104.
- Rubinow, S. I. (1975) *Introduction to Mathematical Biology*, pp 46–100, John Wiley and Sons, Inc., New York.
- Press, W. H., Flannery, B. P., Teukolsky, S. A., and Vetterling, W. T. (1989) *Numerical Recipes: The Art of Scientific Computing (Fortran Version)*, pp 547–572, Cambridge University Press, New York.
- Segel, I. H. (1993) *Enzyme Kinetics: Behavior and Analysis of Rapid Equilibrium and Steady-State Enzyme Systems*, John Wiley and Sons, Inc., New York.
- Shimizu, T., and Johnson, K. A. (1983) *J. Biol. Chem.* 258, 13833–13840.
- Rayment, I. (1996) *J. Biol. Chem.* 271, 15850–15853.
- Cleland, W. W. (1975) *Biochemistry* 14, 3220–3224.
- Roca, J., and Wang, J. C. (1992) *Cell* 71, 833–840.
- Johnson, K. A. (1995) *Methods Enzymol.* 249, 38–61.
- Ali, J. A., Jackson, A. P., Howells, A. J., and Maxwell, A. (1993) *Biochemistry* 32, 2717–2724.
- Tamura, J. K., Bates, A. D., and Gellert, M. (1992) *J. Biol. Chem.* 267, 9214–9222.
- Maxwell, A., and Gellert, M. (1986) *Adv. Protein Chem.* 38, 69–107.
- Bates, A. D., and Maxwell, A. (1989) *EMBO J.* 8, 1861–1866.
- Sugino, A., and Cozzarelli, N. R. (1980) *J. Biol. Chem.* 255, 6299–6306.
- Berger, J. M., Gamblin, S. J., Harrison, S. C., and Wang, J. C. (1996) *Nature* 379, 225–232.

22. Osheroff, N., Zechiedrich, E. L., and Gale, K. C. (1991) *BioEssays* 13, 269–275.
23. Roca, J. (1995) *Trends Biochem. Sci.* 20, 156–160.
24. Sugino, A., Higgins, N. P., Brown, P. O., Peebles, C. L., and Cozzarelli, N. R. (1978) *Proc. Natl. Acad. Sci. U.S.A.* 75, 4838–4842.
25. Mizuuchi, K., Fisher, L. M., O’Dea, M. H., and Gellert, M. (1980) *Proc. Natl. Acad. Sci. U.S.A.* 77, 1847–1851.
26. Orphanides, G., and Maxwell, A. (1994) *Curr. Biol.* 4, 1006–1009.
27. Osheroff, N., Shelton, E. R., and Brutlag, D. L. (1983) *J. Biol. Chem.* 258, 9536–9543.
28. Roca, J., and Wang, J. C. (1994) *Cell* 77, 609–616.
29. Jencks, W. P. (1980) *Adv. in Enzymol. Relat. Areas Mol. Biol.* 51, 75–106.
30. Rodina, M. V., Savelsbergh, A., Katunin, V. I., and Wintermeyer, W. (1997) *Nature* 385, 37–41.
31. Hackney, D. D. (1988) *Proc. Natl. Acad. Sci. U.S.A.* 85, 6314–6318.
32. Boyer, P. D. (1997) *Annu. Rev. Biochem.* 66, 717–749.
33. Hingorani, M. M., Washington, M. T., Moore, K. C., and Patel, S. S. (1997) *Proc. Natl. Acad. Sci. U.S.A.* 94, 5012–5017.
34. Hackney, D. D. (1995) *Nature* 377, 448–450.
35. Gilbert, S. P., Webb, M. R., Brune, M., and Johnson, K. A. (1995) *Nature* 373, 671–676.
36. Wigley, D. B., Davies, G. J., Dodson, E. J., Maxwell, A., and Dodson, G. (1991) *Nature* 351, 624–629.
37. Cabral, J. H. M., Jackson, A. P., Smith, C. V., Shikotra, N., Maxwell, A., and Liddington, R. C. (1997) *Nature* 388, 903–906.
38. Lindsley, J. E., and Wang, J. C. (1993) *Nature* 361, 749–750.

BI9729108